

RANKCLIP: RANKING-CONSISTENT LANGUAGE-IMAGE PRETRAINING

Anonymous authors

Paper under double-blind review

ABSTRACT

Self-supervised contrastive learning models, such as CLIP, have set new benchmarks for vision-language models in many downstream tasks. However, their dependency on rigid one-to-one mappings overlooks the complex and often multifaceted relationships between and within texts and images. To this end, we introduce **RANKCLIP**, a novel pretraining method that extends beyond the rigid one-to-one matching framework of CLIP and its variants. By extending the traditional pair-wise loss to list-wise, and leveraging both in-modal and cross-modal ranking consistency, RANKCLIP improves the alignment process, enabling it to capture the nuanced many-to-many relationships between and within each modality. Through comprehensive experiments, we demonstrate the effectiveness of RANKCLIP in various downstream tasks, notably achieving significant gains in zero-shot classifications over state-of-the-art methods, underscoring the importance of this enhanced learning process.

1 INTRODUCTION

In the realm of computer vision (CV) (Voulodimos et al., 2018), natural language processing (NLP) (Chowdhary & Chowdhary, 2020), and multimodal deep learning (Jabeen et al., 2023; Zhao et al., 2023; Chen et al., 2024a), the alignment between visual and textual modalities (Singh et al., 2022; Chen et al., 2024b) has emerged as a cornerstone for downstream applications, ranging from image captioning (Ghandi et al., 2023) to zero-shot classification (Pourpanah et al., 2022). Contrastive Language-Image Pretraining (CLIP) (Radford et al., 2021) marks a significant advancement in this field, demonstrating incredible performance from training on large amounts of text-image pairs to create self-supervised models that understand (Hendrycks et al., 2021a;b; Chen et al., 2024c) and generate (Ramesh et al., 2021; Crowson et al., 2022) descriptions of visual contents. Following the success of this contrastive learning paradigm, many recent works have been developed upon the original CLIP. More specifically, these enhancements focus on optimizing data efficiency through intrinsic supervision (Li et al., 2021), as well as improving downstream performance via cross-modal late interaction (Yao et al., 2021), hierarchical feature alignment (Gao et al., 2022), geometric consistency regularization (Goel et al., 2022), additional learning (Mu et al., 2022), adaptive loss (Yang et al., 2023), hierarchy-aware attentions (Geng et al., 2023), and softer cross-modal alignment (Gao et al., 2024).

Despite the improvements, these methods often have reliance on strict *pairwise*, *cross-modal*, and *one-to-one* mappings between images and texts, overlooking the actual *many-to-many* relationships that exist both *cross-modal* and *in-modal* in real-world data (Chun, 2023). For example, as shown in Fig. 1, while pretrained models like CLIP can correctly classify `dog`, `cat` and `airplane`, they do not necessarily learn that `dog` and `cat` are more close to each other than `dog` and `airplane`, in terms of both in-modal (`dog` text is more similar to `cat` text than to `airplane` text) and cross-modal (`dog` text is more matched to `cat` image than to `airplane` image) similarities. Because it is rooted from the current contrastive loss that only the correct pairs are optimized while the rest of the unmatched pairs are treated the same, resulting in a large amount of information not used and unknown to the model during and after the training process.

Recognizing the complex *many-to-many* relationships as well as the rich information contained within both *in-modal* and *cross-modal* data, we introduce **Ranking-Consistent Language-Image Pretraining**, (**RANKCLIP**), which employs *ranking consistency* to learn and optimize similarity levels both between (cross-modal) and within (in-modal) the text-image pairs.

054 The concept of ranking consistency stems from
 055 the simple observations that similar texts often
 056 correlate with similar images, as seen with the
 057 dog, cat and airplane example in Fig. 1.
 058 It effectively captures secondary similarity re-
 059 lationships among unmatched pairs, enabling
 060 the model to learn *more efficiently for free*
 061 compared to relying solely on matched pairs.
 062 Ranking consistency is conveniently modeled
 063 as an additional loss term to the traditional con-
 064 trastive loss, requiring no extra external mod-
 065 ules. It acts as a plug-and-play improvement for
 066 many existing methods, including those focus-
 067 ing on data-efficiency (Li et al., 2021), poten-
 068 tially boosting performance in both efficiency
 069 and effectiveness.

069 The main contributions of this paper are: 1)
 070 RANKCLIP, a novel contrastive pretraining
 071 method that uses ranking consistency to exploit
 072 the many-to-many relationships within data, thereby
 073 enhancing performance in downstream tasks such
 074 as zero-shot classification and retrieval accuracy;
 075 and 2) through comprehensive experiments con-
 076 ducted on multiple datasets, we demonstrate the
 077 superior effectiveness of RANKCLIP in improv-
 078 ing pretraining model performance without re-
 079 quiring any additional data or computational re-
 080 sources.

077 2 RELATED WORK

079 Vision-language pretraining has witnessed significant
 080 advancements over the past years (Chen et al.,
 081 2023; Du et al., 2022; Long et al., 2022).
 082 Models such as CLIP (Radford et al., 2021),
 083 ALIGN (Jia et al., 2021) and FLAVA (Singh et al.,
 084 2022) have pioneered the contrastive learning
 085 paradigm applied with text-image pairs, show-
 086 casing remarkable performance and robustness
 087 in downstream tasks. Many follow-up works,
 088 mostly built upon CLIP, have been proposed
 089 since then. Li et al. (2021) introduced DeCLIP,
 090 improving zero-shot performance through in-
 091 trinsic supervision. FILIP (Yao et al., 2021)
 092 advances CLIP’s alignment between image
 093 patches and text with a cross-modal interaction
 094 mechanism. Gao et al. (2022) developed Pyra-
 095 midCLIP, using hierarchical feature alignment
 096 to boost model efficiency and performance. Ad-
 097 ditionally, SLIP (Mu et al., 2022) merges self-
 098 supervised learning with CLIP pre-training for
 099 improved visual representation and accuracy.
 100 Goel et al. (2022) introduced CyCLIP, augmen-
 101 ting CLIP with geometric consistency regulariz-
 102 ers to enhance robustness and performance un-
 103 der varied conditions.

090 Recently, Yang et al. (2023) introduced ALIP,
 091 an adaptive pre-training model that enhances
 092 language-image alignment using raw text and
 093 synthetic captions with dynamic adjustments.
 094 Hi-CLIP (Geng et al., 2023) refines CLIP by
 095 adding hierarchy-aware attentions to uncover
 096 semantic hierarchies in images and texts. Eq-
 097 Sim (Wang et al., 2023) incorporates equivari-
 098 ance loss into vision-language models, signif-
 099 icantly improving sensitivity to semantic changes
 100 in image-text pairs. Additionally, SoftCLIP
 101 (Gao et al., 2024) softens CLIP’s one-to-one
 102 constraint, enabling more flexible cross-modal
 103 alignment through fine-grained adjustments.

097 Compared with existing approaches, RANKCLIP
 098 sets itself apart by fully leveraging the *many-to-*
 099 *many* relationships within each batch of text-
 100 image pairs, promoting learning from both
 101 matched and unmatched pairs with varying
 102 similarities by integrating in-modal and cross-
 103 modal *list-wise ranking consistencies* into the
 104 contrastive training objective. Crucially, RANK-
 105 CLIP diverges from existing models’ pair-wise
 106 training objective by adopting a global, list-
 107 wise optimization approach. In other words,
 108 it considers the rankings of all images and
 109 texts collectively within each batch, rather than
 110 focusing on pairwise similarities as seen in other
 111 methods.

104 3 CLIP PRELIMINARIES

106 CLIP (Radford et al., 2021) has been a prominent
 107 method for learning detailed multimodal repre-
 sentations through the alignment of images and
 texts. Given a set $\mathcal{D} = \{(V_j, T_j)\}_{j=1}^N$ of N image-text

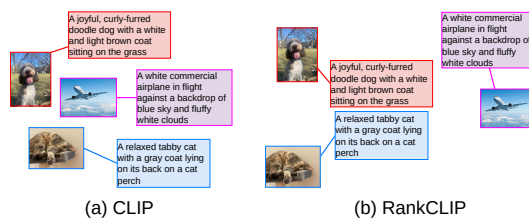


Figure 1: Comparison of learning outcomes between (a) CLIP and (b) RANKCLIP using three text-image pairs: dog (red), cat (blue), and airplane (magenta), where matched pairs share the same color boundaries. CLIP treats all unmatched relationships equally, failing to distinguish similarities better between dog and cat versus airplane. RANKCLIP addresses this by training with ranking consistency, enhancing its understanding of complex relationships.

108 pairs, where V_j denotes an image and T_j is the corresponding text, the goal is to learn representa-
 109 tions that map semantically similar images and texts closer in the embedding space, while dissimilar
 110 pairs are distanced apart. More specifically, the foundational CLIP model employs two encoders:
 111 an image encoder $f_I : \mathcal{I} \rightarrow \mathbb{R}^m$ that processes raw images into visual embeddings and a text en-
 112 coder $f_T : \mathcal{T} \rightarrow \mathbb{R}^n$ which encodes textual data into text embeddings. Then both the text and
 113 visual features are projected to a latent space with identical dimension. Formally, the embeddings
 114 for a text-image pair (V_j, T_j) are denoted as $v_k = f_I(V_j)$ and $t_j = f_T(T_j)$, respectively. The
 115 embeddings are then normalized to lie on an unit hypersphere by enforcing l_2 -norm constraint:

$$116 \hat{v}_j = \frac{v_j}{\|v_j\|_2}, \quad \hat{t}_j = \frac{t_j}{\|t_j\|_2}. \quad (1)$$

117 so that the magnitude information is erased and only direction is preserved.

118 To align the image and text representations, a contrastive loss function, typically a variant of the
 119 InfoNCE loss (Oord et al., 2018), which optimizes the similarity of the matched pair against un-
 120 matched pairs, is utilized, i.e.:

$$121 \mathcal{L}_{\text{CLIP}} = -\frac{1}{2N} \sum_{j=1}^N \left[\underbrace{\log \frac{\exp(\hat{v}_j^\top \hat{t}_j / \tau)}{\sum_{k=1}^N \exp(\hat{v}_j^\top \hat{t}_k / \tau)}}_{\textcircled{1}} + \log \frac{\exp(\hat{t}_j^\top \hat{v}_j / \tau)}{\sum_{k=1}^N \exp(\hat{t}_j^\top \hat{v}_k / \tau)} \right] \quad (2)$$

122 where the first term $\textcircled{1}$ contrasts images with the texts, the second term $\textcircled{2}$ contrasts texts with
 123 the images, and τ denotes a temperature scaling parameter that adjusts the concentration of the
 124 distribution. The optimization of Eqn. (2) results in embeddings where the cosine similarity between
 125 matched image-text pairs is maximized in comparison to unmatched pairs, thus achieving the desired
 126 alignment in the joint embedding space.

127 Despite the efficacy of CLIP in learning correlated multimodal embeddings, it inherently relies on
 128 strict pairwise matched comparisons and fails to capture the more complex, fine-grained nature
 129 of semantic similarity within and across modalities that are generally treated as unmatched. This
 130 observation motivates the development of RANKCLIP, which innovates beyond binary pairwise
 131 contrasts to consider holistic listwise consistency within and across modalities.

132 4 RANKCLIP

133 RANKCLIP efficiently leverages the many-to-many relationships in real-world data by focusing
 134 on both matched and unmatched pairs. As shown in Fig. 2, it not only identifies if an image-
 135 text pair matches but also assesses their relative semantic similarities to other images and texts of
 136 both modalities in the dataset through self-supervised ranking consistency. Uniquely, RANKCLIP
 137 employs a list-wise loss for training batches, distinguishing it from other methods that solely rely on
 138 pair-wise relationships, as discussed in §2.

139 4.1 RANKING MODEL FORMULATION

140 RANKCLIP leverages the Plackett-Luce (PL) ranking model Plackett (1975); Luce (2005); Guiver
 141 & Snelson (2009) to estimate the probability distribution over rankings for every image-text pair
 142 (V_i, T_j) , so that the consistency in their relative ordering with respect to a reference ranking can
 143 be measured. Specifically, for a given data pair, whether it is in-modal (image-image, text-text), or
 144 cross-modal (image-text), we calculate its in- or cross-modal cosine similarity S_{ij} to serve as the
 145 score when measuring the alignment of its ranking with respect to another reference ranking y_{ref} .

146 Following Plackett (1975), we first sort the reference ranking in a descending order to construct the
 147 optimal ranking y^* , and assume that the ego ranking y is sampled from y^* . Thus the probability that
 148 item d with score S_{ij} is ranked k^{th} in the ego ranking y from a set of items \mathcal{D} is the score of $e^{S_{ij}}$
 149 divided by the sum of scores for the items that have not been placed yet:

$$150 \pi(d \mid y_{1:k-1}, y_{\text{ref}}, \mathcal{D}) = \frac{e^{S_{ij}}}{\sum_{d' \in \mathcal{D} \setminus y_{1:k-1}} e^{S_{ij}'}} \quad (3)$$

151 where $y_{1:k-1} = [y_1, y_2, \dots, y_{k-1}]$ denotes the set of items ranked before d . In addition, we propose
 152 a decaying factor $\mu = 1/\log(k+1)$ to scale the loss, so that the top-ranked items can obtain
 153

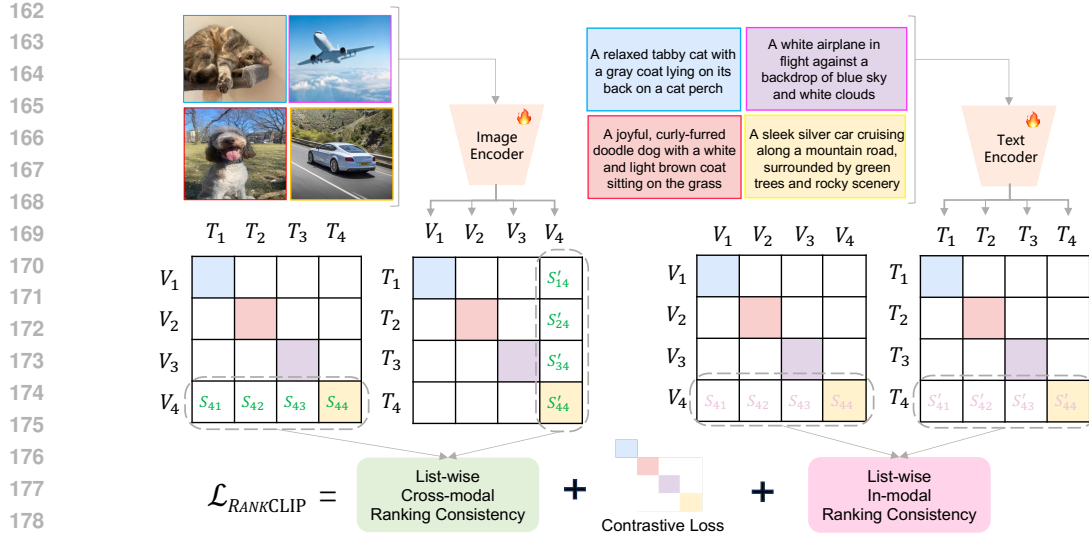


Figure 2: Illustrative overview of RANKCLIP. Unlike conventional contrastive loss, which includes only the middle term, RANKCLIP introduces both cross-modal and in-modal consistency terms by minimizing a self-supervised, list-wise ranking loss. Paired images and texts are indicated by matching contour line colors. V , T , and S represent image embeddings, text embeddings, and similarity scores, respectively.

higher weights: Consequently, the probability of the entire ranking y is the product of all individual placement probabilities:

$$\mathcal{P}(y, y_{\text{ref}}) = \prod_{k=1}^K \mu \cdot \pi(y_k | y_{1:k-1}, \mathbf{y}_{\text{ref}}, \mathcal{D}). \quad (4)$$

RANKCLIP’s objective is to maximize the consistency log-likelihood of the list ranking in one modality towards the reference ranking (from the same/in-modal and different/cross-modal data), which conveniently aligns with minimizing the negative log-likelihood loss:

$$\mathcal{L}_{\text{PL}} = -\log \mathcal{P}(y, y_{\text{ref}}) \quad (5)$$

4.2 CROSS-MODAL CONSISTENCY RANKING

As illustrated by the green box in Fig. 2, RANKCLIP utilizes secondary relationships between unmatched visual and textual representations by constructing a list-wise rank loss. This approach ensures that the semantic similarity rankings between one image and multiple texts align with those between one corresponding text and multiple images. For example, as shown in Fig. 1, from the dog perspective, the semantic distance between dog image and cat text is closer compared to the plane text. This relationship should also apply between the dog text and the cat, plane images. Mathematically, Eq. (5) can be specified as:

$$\mathcal{L}_{\text{cross-modal}} = -\log \mathcal{P}(\mathbf{y}_{\text{image-text}}, \mathbf{y}_{\text{text-image}}) \quad (6)$$

$$= -\log \mathcal{P}(\hat{\mathbf{v}} \cdot \hat{\mathbf{t}}^{\text{T}}, \hat{\mathbf{t}} \cdot \hat{\mathbf{v}}^{\text{T}}) \quad (7)$$

By optimizing Eq. (6), RANKCLIP enhances its ability to bridge the semantic gap between modalities by leveraging nuanced unmatched correlations. This can also be viewed as learning a symmetric cosine-similarity matrix, further reinforcing semantic consistency across modalities.

4.3 IN-MODAL CONSISTENCY RANKING

The pink box in Fig. 2 highlights the in-modal consistency component of the proposed rank loss. RANKCLIP ensures semantic consistency within each modality – image to image and text to text – enhancing the use of secondary unmatched relationships as an optimization objective. The underlying principle is that similar images should correspond to similar texts. For example, in Fig. 1, from the dog image perspective, the cat image is the most similar, followed by the plane image. This

relationship should hold true for their corresponding texts as well, where we utilize this to construct our y and y_{ref} from Eq. (5). Mathematically, Eq. (5) can be specified as:

$$\mathcal{L}_{\text{in-modal}} = -\log \mathcal{P}(\mathbf{y}_{\text{text-text}}, \mathbf{y}_{\text{image-image}}) \quad (8)$$

$$= -\log \mathcal{P}(\hat{\mathbf{t}} \cdot \hat{\mathbf{t}}^{\mathbf{T}}, \hat{\mathbf{v}} \cdot \hat{\mathbf{v}}^{\mathbf{T}}) \quad (9)$$

where $\hat{\mathbf{t}}$ and $\hat{\mathbf{v}}$ are the text and image batch embedding matrix, respectively. Via Eq. (8), the model can efficiently leverage the nuanced in-modal relationships to learn a richer and more structured semantic representation.

4.4 RANKCLIP LOSS

Combining both cross-modal and in-modal consistency with the traditional contrastive loss (more details in Appendix 3), the complete rank loss is thus formulated as:

$$\mathcal{L}_{\text{RANKCLIP}} = \mathcal{L}_{\text{CLIP}} + \lambda_1 \mathcal{L}_{\text{in-modal}} + \lambda_2 \mathcal{L}_{\text{cross-modal}} \quad (10)$$

which is also depicted in Fig. 2. By supplementing the pairwise contrastive loss with cross-modal and in-modality ranking consistency loss, RANKCLIP systematically organizes embeddings to fully exploit both global and fine-grained secondary unmatched relationships, which enhances the learning of more informative and accurate representations, better supporting downstream multi-modal tasks. The complete RANKCLIP is detailed in Algorithm 1.

Algorithm 1 Pseudo-code of RANKCLIP loss in a Python-like style.

```

241 # emb_pred: predictions from the model, shape [embs_length, embs_length]
242 # emb_true: ground truth labels, shape [embs_length, embs_length]
243
244 def rank_loss(emb_pred, emb_true):
245     # Shuffle for randomised tie resolution
246     emb_pred_shuff = emb_pred[:, random_indices]
247     emb_true_shuff = emb_true[:, random_indices]
248     # Record the rank label index
249     emb_true_sorted, indices = emb_true_shuff.sort(descending=True, dim
250     ==-1)
251     # Ranking the pred embedding by the true indices
252     preds_sorted = gather(emb_pred_shuff, dim=1, index=indices)
253     # Implementation of the Eq.1, Eq.2 and Eq.3
254     max_pred_values, _ = preds_sorted.max(dim=1, keepdim=True)
255     preds_sorted_minus_max = preds_sorted - max_pred_values
256     cumsums = cumsum(preds_sorted_minus_max.exp().flip(dims=[1]), dim=1).
257     flip(dims=[1])
258     loss = (log(cumsums) - preds_sorted_minus_max) * scale_factor
259     return mean(sum(loss, dim=1))
260
261 # Cross-modal embeddings
262 logits_text_per_image=image_embeds @ text_embeds.T
263 logits_image_per_text=logits_text_per_image.T
264 # In-modal embeddings
265 logits_image_per_image=image_embeds @ image_embeds.T
266 logits_text_per_text=text_embeds @ text_embeds.T
267 # Compute the cross-modal rank loss
268 Cross_modal_loss=rank_loss(logits_text_per_image,logits_image_per_text)+
269     rank_loss(logits_image_per_text, logits_text_per_image)
270 # Compute the in-modal rank loss
271 In_modal_loss=rank_loss(logits_image_per_image,logits_text_per_text)+
272     rank_loss(logits_text_per_text, logits_image_per_image)
273 # Rank loss
274 Rank_loss=Contrastive_loss+Cross_modal_loss+In_modal_loss

```

Table 1: Zero-shot top-1, top-3 and top-5 classification accuracy on CIFAR-10, CIFAR-100 and ImageNet1K. Relative to CLIP, RANKCLIP achieves higher accuracy with *average* top-1, top-3, and top-5 improvements of **+2.46%**, **+2.25%**, and **+2.40%**, respectively. RANKCLIP also outperforms ALIP consistently across the datasets.

	CIFAR-10			CIFAR-100			ImageNet1K		
	Top1	Top3	Top5	Top1	Top3	Top5	Top1	Top3	Top5
CLIP	36.35%	70.28%	85.02%	12.22%	24.93%	33.56%	12.08%	21.86%	27.48%
ALIP	35.71%	72.39%	88.77%	13.67%	27.10%	34.76%	15.62%	26.90%	32.50%
RANKCLIP	37.03% (+0.68%)	67.67% (-2.61%)	83.09% (-1.93%)	13.98% (+1.76%)	27.70% (+2.77%)	36.17% (+2.61%)	17.02% (+4.94%)	28.44% (+6.58%)	33.99% (+6.51%)

Table 2: Zero-shot top-1, top-3 and top-5 classification accuracy on variants of ImageNet1K that have *natural distribution shifts*. Relative to CLIP, RANKCLIP achieves higher accuracy with *average* top-1, top-3, and top-5 improvements of **+3.15%**, **+4.19%**, and **+4.66%**, respectively. Notice that the average improvements are more significant than when tested on ImageNet1K without distribution shift, indicating better robustness.

	ImageNetV2			ImageNetSketch			ImageNet-A			ImageNet-R		
	Top1	Top3	Top5	Top1	Top3	Top5	Top1	Top3	Top5	Top1	Top3	Top5
CLIP	12.11%	22.66%	28.57%	3.20%	7.00%	9.83%	3.16%	8.81%	13.04%	11.34%	21.38%	27.10%
ALIP	15.62%	27.34%	32.82%	5.10%	10.37%	14.01%	3.53%	9.14%	13.61%	14.25%	25.74%	32.43%
RANKCLIP	17.03% (+4.92%)	28.60% (+5.94%)	34.18% (+5.61%)	5.82% (+2.62%)	11.35% (+4.35%)	14.87% (+5.04%)	3.82% (+0.66%)	9.16% (+0.35%)	13.77% (+0.73%)	15.74% (+4.40%)	27.51% (+6.13%)	34.36% (+7.26%)

5 EXPERIMENTS

5.1 EXPERIMENTAL SETUP

Baselines. The most direct baseline to RANKCLIP is the original CLIP (Radford et al., 2021). In addition, to further demonstrate the superior performance of RANKCLIP, we include ALIP (Yang et al., 2023), which leverages synthetic captions to enhance vision-language representation learning. More specifically, it employs a unique architecture that dynamically adjusts sample and pair weights to mitigate the impact of noisy or irrelevant data, which is quite orthogonal to our approach. The training procedures and parameters of all models are detailed in Appendix A.

Pretraining dataset. Both baseline models, CLIP (Radford et al., 2021), ALIP (Yang et al., 2023) and the proposed RANKCLIP are pretrained on the Conceptual Captions 3M (CC3M) dataset (Sharma et al., 2018), which contains around 3.3 million text-image pairs. Despite being much smaller than CLIP’s initial dataset (Ilharco et al., 2021), CC3M effectively supports the development of pretrained models with strong zero-shot capabilities and is widely used in existing language-image pretraining research (Carlini & Terzis, 2021; Li et al., 2021; Tejankar et al., 2021; Mu et al., 2022; Goel et al., 2022). Additionally, as discussed later in §6.2, we trained both CLIP and RANKCLIP on 15 million text-image pairs, filtered from YFCC100M (Thomee et al., 2016), referred to as YFCC15M, to conduct an ablation study on the impact of data size.

5.2 ZERO-SHOT CLASSIFICATION

Zero-shot capability is one of the most significant improvements that CLIP achieves. Thus in this section, we first evaluate the zero-shot classification performance of CLIP, ALIP and the proposed RANKCLIP. Following (Goel et al., 2022), we conduct our experiments on CIFAR-10 (Krizhevsky et al., 2009), CIFAR-100 (Krizhevsky et al., 2009), and ImageNet1K (Deng et al., 2009; Russakovsky et al., 2015) dataset.

As shown in Table 1, RANKCLIP consistently outperforms CLIP across CIFAR-10, CIFAR-100, and ImageNet1K datasets. Relative to CLIP, RANKCLIP shows average improvements of **+3.15%**, **+4.19%**, and **+4.66%** in top-1, top-3 and top-5 metrics, respectively. Particularly on the more challenging ImageNet1K dataset, RANKCLIP improves relative top-1 accuracy by **+4.94%** over CLIP, highlighting the effectiveness of the proposed ranking consistency in enhancing language-image alignment and understanding with the same amount of training data. The two cases where RANKCLIP does not excel are the top-3 and top-5 accuracy on CIFAR-10. However, this is likely

Table 3: Linear probing top-1 accuracy on 11 downstream datasets. RANKCLIP achieves higher accuracy than CLIP with an average improvement of **+1.30%**. RANKCLIP also outperforms ALIP, although less significantly.

	CIFAR-10	CIFAR-100	DTD	FGVG-Aircraft	Food101	GTSRB	Imagenet1K	OxfordPets	SST2	STL10	SVHN	Average
CLIP	72.40%	48.43%	49.89%	26.10%	48.59%	65.20%	77.49%	49.74%	53.71%	83.59%	44.80%	56.37%
ALIP	73.87%	51.00%	58.09%	27.72%	49.74%	60.34%	73.14%	59.36%	53.98%	87.94%	38.07%	57.56%
RANKCLIP	72.54%	49.16%	53.24%	24.99%	47.11%	63.37%	86.40%	54.10%	54.09%	86.10%	43.30%	57.67%
	(+0.14%)	(+0.73%)	(+3.35%)	(-1.11%)	(-1.48%)	(-1.83%)	(+8.91%)	(+4.36%)	(+0.38%)	(+2.51%)	(-1.50%)	(+1.30%)

Table 4: Zero-shot image and text retrievals on Flickr30K and MSCOCO. RANKCLIP achieves higher accuracy than both CLIP and ALIP on most cases.

	Flickr30K						MSCOCO					
	Text Retrieval			Image Retrieval			Text Retrieval			Image Retrieval		
	R@1	R@5	R@10	R@1	R@5	R@10	R@1	R@5	R@10	R@1	R5	R@10
CLIP	84.00%	88.70%	91.00%	8.70%	16.90%	21.20%	82.06%	85.24%	87.82%	5.04%	12.98%	18.32%
ALIP	84.40%	90.00%	92.50%	9.40%	17.60%	21.30%	82.56%	86.04%	88.26%	6.08%	13.96%	19.38%
RANKCLIP	84.10%	89.40%	91.90%	8.10%	16.40%	21.70%	82.90%	85.68%	88.00%	5.60%	13.20%	18.02%
	(+0.10%)	(+0.70%)	(+0.90%)	(-0.60%)	(-0.50%)	(+0.50%)	(+0.84%)	(+0.44%)	(+0.18%)	(+0.56%)	(+0.22%)	(-0.30%)

because CIFAR-10 with top-3 and top-5 metrics is much simpler, reducing the demand for a deeper model understanding.

Additionally, we observe that RANKCLIP consistently outperforms ALIP, suggesting that our ranking consistency more effectively enhances text-image representations and alignments compared to the synthetic captions proposed in ALIP. Another trend we observe is that RANKCLIP shows the most significant improvement in top-1 accuracy compared to top-3 and top-5. Considering the real-world emphasis on the topmost model output, RANKCLIP is likely to offer considerable advantages in practical applications.

5.3 ROBUSTNESS TO DISTRIBUTION SHIFTS

To evaluate the robustness of RANKCLIP under distribution shifts, we test it alongside CLIP and ALIP across four ImageNet variants, including ImageNetV2 (Recht et al., 2019), ImageNetSketch (Wang et al., 2019), ImageNet-A (Hendrycks et al., 2021b), and ImageNet-R (Hendrycks et al., 2021a), which are designed to assess resilience to different distribution shifts.

As shown in Table 2, RANKCLIP outperforms both CLIP and ALIP consistently. Notably, relative to CLIP, RANKCLIP’s accuracy improvements in shifted conditions are **+3.15%** (top-1), **+4.19%** (top-3), and **+4.66%** (top-5), surpassing its performance in standard settings (Table 1) of **+2.46%** (top-1), **+2.25%** (top-3), and **+2.40%** (top-5), indicating the even more superior performance in robustness under distribution shifts.

5.4 LINEAR PROBING

We also evaluate whether the introduced ranking consistency retains its advantages when supplemented with additional in-domain supervision. Specifically, we use linear probing, where the pretrained encoders from CLIP, ALIP, and RANKCLIP remain unchanged while a logistic regression classifier is trained on domain-specific datasets. We evaluate on a suite of 11 standard image classification datasets as our in-domain datasets, which include CIFAR-10, CIFAR-100, Describable Textures Dataset (DTD) (Cimpoi et al., 2014), Fine-Grained Visual Classification of Aircraft (FGVG-Aircraft) (Maji et al., 2013), Food101 (Bossard et al., 2014), German Traffic Sign Detection Benchmark (GTSDB) (Stallkamp et al., 2012), ImageNet1K (Deng et al., 2009; Russakovsky et al., 2015), OxfordPets (Parkhi et al., 2012), Stanford Sentiment Treebank v2 (SST2) (Socher et al., 2013), STL-10 (Coates et al., 2011), and Street View House Numbers (SVHN) (Netzer et al., 2011) dataset.

Table 3 indicates that RANKCLIP consistently outperforms CLIP, with relative improvements ranging from **+0.14%** to **+8.91%** and an average accuracy increase of **+1.30%**. When compared to ALIP, RANKCLIP also shows better performance on average, though the gains are relatively modest.

Table 5: Ablation zero-shot classification accuracy of cross-modal-only model RANKCLIP_C and in-modal-only model RANKCLIP_I on CIFAR-10, CIFAR-100 and ImageNet1K datasets. Bold indicates the best performance, while blue indicates the second best.

	CIFAR-10			CIFAR-100			ImageNet1K		
	Top1	Top3	Top5	Top1	Top3	Top5	Top1	Top3	Top5
CLIP	36.35%	70.28%	85.02%	12.22%	24.93%	33.56%	12.08%	21.86%	27.48%
RANKCLIP	37.03%	67.67%	83.09%	13.98%	27.70%	36.17%	17.02%	28.44%	33.99%
RANKCLIP _I	37.47%	69.89%	84.53%	13.89%	27.34%	35.90%	16.66%	27.63%	33.15%
RANKCLIP _C	28.26%	59.65%	75.45%	13.29%	26.85%	34.71%	16.98%	28.25%	33.90%

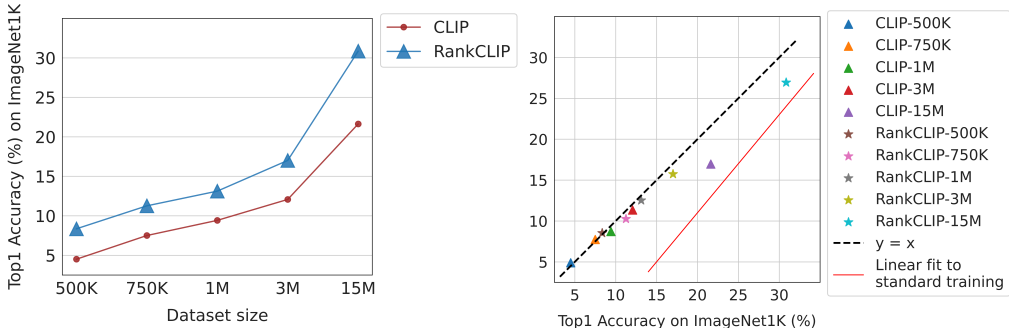


Figure 3: Ablation studies of CLIP and RANKCLIP trained with different data sizes. *Left*: zero-shot top-1 classification accuracy on ImageNet1K with various data sizes randomly sampled from CC3M. RANKCLIP consistently outperforms CLIP with significant margins. *Right*: zero-shot top-1 classification accuracy on ImageNet1K (horizontal axis) and ImageNet1K-R (vertical axis). RANKCLIP demonstrates better robustness as well as accuracy.

5.5 ZERO-SHOT IMAGE-TEXT RETRIEVAL

In the final part of our experiments, we assess RANKCLIP on zero-shot cross-modal retrieval tasks (image-to-text and text-to-image) using the Flickr30k (Plummer et al., 2015) and MSCOCO (Lin et al., 2014) datasets. As shown in Table 4, RANKCLIP generally outperforms the two baseline methods, though improvements are less significant compared to earlier results in Table 1, Table 2 and Table 3. The relatively modest gains in retrieval tasks may stem from the complex requirements of discerning image-text similarities across varying resolutions and object details, a significant departure from the simpler demands of image classification tasks. Despite this, the overall improvement highlights RANKCLIP’s advantage, thanks to the deeper insights provided by ranking consistency in the language-image training process.

6 ABLATION STUDIES

6.1 ABLATION ON LOSS COMPONENTS

To further assess the effectiveness of the proposed ranking consistency, we developed two variants of RANKCLIP: RANKCLIP_C, focusing solely on cross-modal consistency with $\lambda_i = 0$, and RANKCLIP_I, emphasizing in-modal consistency with $\lambda_c = 0$. Both models underwent the same pretraining as outlined in Appendix A and were tested in a zero-shot classification experiment on ImageNet1K as in §5.2. The results are shown in Table 5, with bold font indicating the best performance, and blue color representing the second best results. We can see that, while RANKCLIP achieves the best performance, both RANKCLIP_C and RANKCLIP_I demonstrate notable improvements over CLIP. Interestingly, RANKCLIP_I matches the performance of RANKCLIP_C, highlighting the often-underestimated value of in-modal consistency in enhancing model effectiveness.

6.2 ABLATION ON DATA SIZES

To evaluate the scalability of RANKCLIP, we trained both CLIP and RANKCLIP using 500K, 750K, 1M, and 3M text-image pairs from the CC3M dataset and 15M text-image pairs from the

Table 6: Linear probing top-1 accuracy on 10 downstream datasets. RANKCLIP achieves higher accuracy than CLIP with an average improvement of +5.03% after pretrained on YFCC15M dataset. The results further demonstrate the potential of our approach for applications on large-scale datasets.

	CIFAR-10	CIFAR-100	DTD	FGVG-Aircraft	Food101	GTSRB	OxfordPets	SST2	STL10	SVHN	Average
CLIP-15M	78.72%	56.46%	61.70%	25.44%	61.65%	68.69%	60.78%	55.24%	89.95%	47.98%	60.66%
RANKCLIP-15M	83.21% (+4.49%)	62.36% (+5.90%)	66.06% (+4.36%)	32.25% (+6.81%)	68.09% (+6.44%)	74.14% (+5.45%)	67.40% (+6.62%)	56.23% (+0.99%)	94.15% (+4.20%)	53.03% (+5.05%)	65.69% (+5.03%)

YFCC15M dataset following the same procedure detailed in Appendix A. Fig. 3 left presents the zero-shot top-1 classification accuracy on ImageNet1K, where RANKCLIP consistently outperforms CLIP. Notably, it shows a *greater performance increments* as dataset size grows from 1M to 15M pairs, suggesting RANKCLIP’s superior scalability, a critical attribute for language-image pretraining. Furthermore, as shown in Table 6, we conducted linear probing on RANKCLIP and CLIP, both pretrained on the 15M text-image pairs, to demonstrate the more promising potential of our method on large-scale datasets.

Fig. 3 right illustrates RANKCLIP’s robustness across different dataset sizes. The horizontal axis shows the top-1 accuracy on standard ImageNet1K, and the vertical axis on ImageNet1K-R, with a black diagonal line ($y = x$) representing ideal robustness. Any deviation below this line indicates reduced robustness. RANKCLIP consistently stays well above both the red baseline, which reflects typical in-distribution to out-of-distribution generalization (Miller et al., 2021), and close to the ideal line, demonstrating exceptional robustness to distribution shifts.

7 ANALYSIS

7.1 MODALITY GAP

In this section, we analyze the modality gaps of CLIP and our proposed RANKCLIP by visualizing 250 text-image pair embeddings, reduced to two dimensions using UMAP (McInnes et al., 2018), and complement this with a histogram of the gaps. Modality gap (Liang et al., 2022) refers to a geometric phenomenon observed in the representation spaces of multimodal models, where different data modalities (like images and texts) are embedded at a noticeable distance from each other, rather than being uniformly distributed as ideally expected. This gap, inherent from initialization and preserved during the contrastive learning process like in CLIP, poses a challenge in language-image pretraining by impacting joint data modeling and understanding. Recent studies (Srivastava & Sharma, 2024; Kumar & Martinen, 2024; Oh et al., 2024) suggest that reducing this gap could enhance multimodal representations and downstream task performance. The results shown in Fig. 4 indicate that RANKCLIP exhibits a significantly smaller modality gap than CLIP, demonstrating that our ranking consistency approach effectively enhances understanding of text-image semantics.

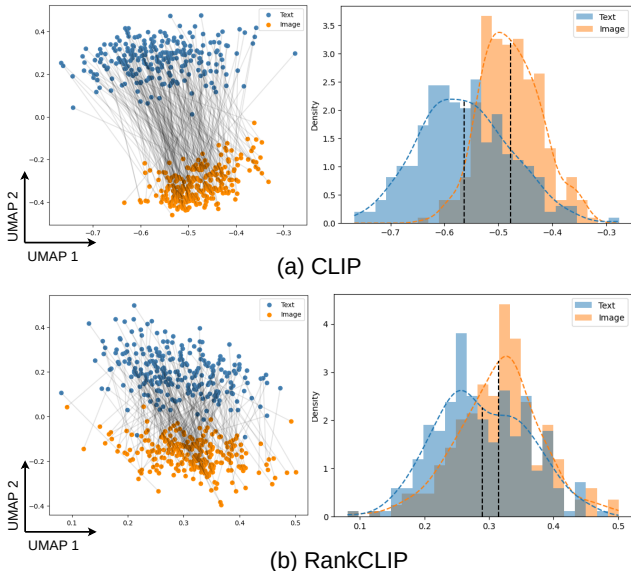


Figure 4: Scatter and histograms plots illustrating modality gaps of (a) CLIP and (b) RANKCLIP.

7.2 ALIGNMENT AND UNIFORMITY

Besides alleviating modality gap, it is also commonly believed that a successful contrastive learning method should as well ensure a *broad* and *uniform* distribution covering an hypersphere in space (Wang & Isola, 2020). These two goals, characterized as similarity and uniformity, can be assessed with alignment and uniformity scores, respectively. More specifically, following Goel et al. (2022) and notations defined in §4, we calculate the alignment score S_A , and uniformity score S_U to be:

$$S_A = \frac{1}{N} \sum_{j=1}^N \hat{I}_j^T \hat{T}_j, \quad (11)$$

$$S_U = \log \left(\frac{1}{N(N-1)} \sum_{j=1}^N \sum_{k=1, j \neq k}^N \exp^{-\hat{I}_j^T \hat{T}_k} \right) \quad (12)$$

where N is the total number of text-image pairs. Essentially, S_A represents the averaged cosine similarity between text and image embeddings, and S_U averages the dissimilarity measures (exponentiated negative dot products) between all unique pairs of text-image embeddings in the dataset, quantifying how evenly these embeddings are distributed.

A high alignment score represents a strong correlation or similarity between pairs of text-image embeddings, indicating that the images and their textual descriptions are closely aligned in the embedding space. Conversely, a high uniformity score suggests that embeddings are not uniformly distributed; they may be clustering together or not utilizing the embedding space efficiently, which can indicate redundancy in the representations or a lack of diversity. A low uniformity score, on the other hand, suggests that the embeddings are well spread out across the space, indicating a diverse and efficient use of the embedding space, which is generally desirable for tasks like retrieval, where a wide coverage of possible queries are preferred.

As shown in Table 7, we observe that, although CLIP learns representations that are better aligned, as evidenced by its top-ranking alignment scores, these representations fail to achieve uniform distribution across the hypersphere, as highlighted by its significantly higher absolute uniformity scores.

On the other hand, RANKCLIP, along with two of its ablated version, RANKCLIP_I and RANKCLIP_C, presents much better balance between alignment and uniformity, which results in improved downstream task performance as illustrated in previous experiments as well as in the representative ZS-Top1 results in Table 7. We also find the results to be informative on a higher level where it indicates that optimizing contrastive learning towards single objective such as alignment or uniformity would not intuitively result in higher downstream task performance.

Table 7: Alignment and uniformity scores of CLIP, RANKCLIP, and its two ablated variants.

	CIFAR-10			CIFAR-100			ImageNet1K		
	S_A	S_U	ZS-Top1	S_A	S_U	ZS-Top1	S_A	S_U	ZS-Top1
CLIP	0.40	-0.35	36.35%	0.42	-0.35	12.22%	0.44	-0.29	12.08%
RANKCLIP	0.23	-0.17	37.03%	0.26	-0.16	13.98%	0.33	-0.11	17.02%
RANKCLIP _I	0.24	-0.16	37.47%	0.26	-0.15	13.89%	0.32	-0.10	16.66%
RANKCLIP _C	0.18	-0.12	28.26%	0.18	-0.10	13.29%	0.26	-0.09	16.98%

8 CONCLUSION

In this paper, we introduce RANKCLIP, a novel language-image pretraining method that integrates ranking consistency into the contrastive learning paradigm. RANKCLIP aims to better understand the complex many-to-many relationships in diverse text-image pairs by optimizing a self-supervised, list-wise rank loss. Through extensive experiments, including zero-shot classification, robustness to distribution shifts, linear probing, and zero-shot image-text retrieval, RANKCLIP not only enhances performance but also improves model robustness and semantic comprehension, outperforming the baseline CLIP and another state-of-the-art model ALIP. Our ablation studies and analyses further demonstrate and interpret the significance of each component of RANKCLIP in boosting performance and understanding across modalities. We believe that the methodologies and principles of RANKCLIP will inspire further research and lead to the development of models with a deeper understanding of the intricate interactions between visual and textual data.

REFERENCES

- 540
541
542 Lukas Bossard, Matthieu Guillaumin, and Luc Van Gool. Food-101 – mining discriminative com-
543 ponents with random forests. In *European Conference on Computer Vision*, 2014.
- 544
545 Nicholas Carlini and Andreas Terzis. Poisoning and backdooring contrastive learning. *arXiv preprint*
546 *arXiv:2106.09667*, 2021.
- 547
548 Fei-Long Chen, Du-Zhen Zhang, Ming-Lun Han, Xiu-Yi Chen, Jing Shi, Shuang Xu, and Bo Xu.
549 Vlp: A survey on vision-language pre-training. *Machine Intelligence Research*, 20(1):38–56,
550 2023.
- 551
552 Zhaorun Chen, Yichao Du, Zichen Wen, Yiyang Zhou, Chenhang Cui, Zhenzhen Weng, Haoqin
553 Tu, Chaoqi Wang, Zhengwei Tong, Qinglan Huang, et al. Mj-bench: Is your multimodal reward
554 model really a good judge for text-to-image generation? *arXiv preprint arXiv:2407.04842*, 2024a.
- 555
556 Zhaorun Chen, Zhuokai Zhao, Hongyin Luo, Huaxiu Yao, Bo Li, and Jiawei Zhou. Halc: Object
557 hallucination reduction via adaptive focal-contrast decoding. *arXiv preprint arXiv:2403.00425*,
558 2024b.
- 559
560 Zhaorun Chen, Zhuokai Zhao, Zhihong Zhu, Ruiqi Zhang, Xiang Li, Bhiksha Raj, and Huaxiu Yao.
561 Autopr: Automating procedural supervision for multi-step reasoning via controllable question
562 decomposition. *arXiv preprint arXiv:2402.11452*, 2024c.
- 563
564 KR1442 Chowdhary and KR Chowdhary. Natural language processing. *Fundamentals of artificial*
565 *intelligence*, pp. 603–649, 2020.
- 566
567 Sanghyuk Chun. Improved probabilistic image-text representations. *arXiv preprint*
568 *arXiv:2305.18171*, 2023.
- 569
570 M. Cimpoi, S. Maji, I. Kokkinos, S. Mohamed, , and A. Vedaldi. Describing textures in the wild. In
571 *Proceedings of the IEEE Conf. on Computer Vision and Pattern Recognition (CVPR)*, 2014.
- 572
573 Adam Coates, Andrew Ng, and Honglak Lee. An analysis of single-layer networks in unsupervised
574 feature learning. In *Proceedings of the fourteenth international conference on artificial intelli-*
575 *gence and statistics*, pp. 215–223. JMLR Workshop and Conference Proceedings, 2011.
- 576
577 Katherine Crowson, Stella Biderman, Daniel Kornis, Dashiell Stander, Eric Hallahan, Louis Cas-
578 tricato, and Edward Raff. Vqgan-clip: Open domain image generation and editing with natural
579 language guidance. In *European Conference on Computer Vision*, pp. 88–105. Springer, 2022.
- 580
581 Jia Deng, Wei Dong, Richard Socher, Li-Jia Li, Kai Li, and Li Fei-Fei. Imagenet: A large-scale hi-
582 erarchical image database. In *2009 IEEE conference on computer vision and pattern recognition*,
583 pp. 248–255. Ieee, 2009.
- 584
585 Jacob Devlin, Ming-Wei Chang, Kenton Lee, and Kristina Toutanova. Bert: Pre-training of deep
586 bidirectional transformers for language understanding. *arXiv preprint arXiv:1810.04805*, 2018.
- 587
588 Yifan Du, Zikang Liu, Junyi Li, and Wayne Xin Zhao. A survey of vision-language pre-trained
589 models. *arXiv preprint arXiv:2202.10936*, 2022.
- 590
591 Yuting Gao, Jinfeng Liu, Zihan Xu, Jun Zhang, Ke Li, Rongrong Ji, and Chunhua Shen. Pyramid-
592 clip: Hierarchical feature alignment for vision-language model pretraining. *Advances in neural*
593 *information processing systems*, 35:35959–35970, 2022.
- 594
595 Yuting Gao, Jinfeng Liu, Zihan Xu, Tong Wu, Enwei Zhang, Ke Li, Jie Yang, Wei Liu, and Xing
596 Sun. Softclip: Softer cross-modal alignment makes clip stronger. In *Proceedings of the AAAI*
597 *Conference on Artificial Intelligence*, volume 38, pp. 1860–1868, 2024.
- 598
599 Shijie Geng, Jianbo Yuan, Yu Tian, Yuxiao Chen, and Yongfeng Zhang. Hiclip: Contrastive
600 language-image pretraining with hierarchy-aware attention. *arXiv preprint arXiv:2303.02995*,
601 2023.

- 594 Taraneh Ghandi, Hamidreza Pourreza, and Hamidreza Mahyar. Deep learning approaches on image
595 captioning: A review. *ACM Computing Surveys*, 56(3):1–39, 2023.
- 596
- 597 Shashank Goel, Hritik Bansal, Sumit Bhatia, Ryan Rossi, Vishwa Vinay, and Aditya Grover. Cy-
598 clip: Cyclic contrastive language-image pretraining. *Advances in Neural Information Processing*
599 *Systems*, 35:6704–6719, 2022.
- 600 John Guiver and Edward Snelson. Bayesian inference for plackett-luce ranking models. In *proceed-*
601 *ings of the 26th annual international conference on machine learning*, pp. 377–384, 2009.
- 602
- 603 Kaiming He, Xiangyu Zhang, Shaoqing Ren, and Jian Sun. Deep residual learning for image recog-
604 nition. In *Proceedings of the IEEE conference on computer vision and pattern recognition*, pp.
605 770–778, 2016.
- 606 Dan Hendrycks, Steven Basart, Norman Mu, Saurav Kadavath, Frank Wang, Evan Dorundo, Rahul
607 Desai, Tyler Zhu, Samyak Parajuli, Mike Guo, et al. The many faces of robustness: A criti-
608 cal analysis of out-of-distribution generalization. In *Proceedings of the IEEE/CVF international*
609 *conference on computer vision*, pp. 8340–8349, 2021a.
- 610 Dan Hendrycks, Kevin Zhao, Steven Basart, Jacob Steinhardt, and Dawn Song. Natural adversarial
611 examples. In *Proceedings of the IEEE/CVF conference on computer vision and pattern recogni-*
612 *tion*, pp. 15262–15271, 2021b.
- 613
- 614 Gabriel Ilharco, Mitchell Wortsman, Ross Wightman, Cade Gordon, Nicholas Carlini, Rohan Taori,
615 Achal Dave, Vaishaal Shankar, Hongseok Namkoong, John Miller, Hannaneh Hajishirzi, Ali
616 Farhadi, and Ludwig Schmidt. Openclip, July 2021. URL [https://doi.org/10.5281/](https://doi.org/10.5281/zenodo.5143773)
617 [zenodo.5143773](https://doi.org/10.5281/zenodo.5143773). If you use this software, please cite it as below.
- 618 Summaira Jabeen, Xi Li, Muhammad Shoib Amin, Omar Bourahla, Songyuan Li, and Abdul Jab-
619 bar. A review on methods and applications in multimodal deep learning. *ACM Transactions on*
620 *Multimedia Computing, Communications and Applications*, 19(2s):1–41, 2023.
- 621
- 622 Chao Jia, Yinfei Yang, Ye Xia, Yi-Ting Chen, Zarana Parekh, Hieu Pham, Quoc Le, Yun-Hsuan
623 Sung, Zhen Li, and Tom Duerig. Scaling up visual and vision-language representation learning
624 with noisy text supervision. In *International conference on machine learning*, pp. 4904–4916.
625 PMLR, 2021.
- 626 Alex Krizhevsky, Geoffrey Hinton, et al. Learning multiple layers of features from tiny images.
627 2009.
- 628
- 629 Yogesh Kumar and Pekka Marttinen. Improving medical multi-modal contrastive learning with
630 expert annotations. *arXiv preprint arXiv:2403.10153*, 2024.
- 631 Yangguang Li, Feng Liang, Lichen Zhao, Yufeng Cui, Wanli Ouyang, Jing Shao, Fengwei Yu,
632 and Junjie Yan. Supervision exists everywhere: A data efficient contrastive language-image pre-
633 training paradigm. *arXiv preprint arXiv:2110.05208*, 2021.
- 634
- 635 Victor Weixin Liang, Yuhui Zhang, Yongchan Kwon, Serena Yeung, and James Y Zou. Mind the
636 gap: Understanding the modality gap in multi-modal contrastive representation learning. *Ad-*
637 *vances in Neural Information Processing Systems*, 35:17612–17625, 2022.
- 638 Tsung-Yi Lin, Michael Maire, Serge Belongie, James Hays, Pietro Perona, Deva Ramanan, Piotr
639 Dollár, and C Lawrence Zitnick. Microsoft coco: Common objects in context. In *Computer*
640 *Vision—ECCV 2014: 13th European Conference, Zurich, Switzerland, September 6–12, 2014,*
641 *Proceedings, Part V 13*, pp. 740–755. Springer, 2014.
- 642
- 643 Siqu Long, Feiqi Cao, Soyeon Caren Han, and Haiqin Yang. Vision-and-language pretrained mod-
644 els: A survey. *arXiv preprint arXiv:2204.07356*, 2022.
- 645 R Duncan Luce. *Individual choice behavior: A theoretical analysis*. Courier Corporation, 2005.
- 646
- 647 S. Maji, J. Kannala, E. Rahtu, M. Blaschko, and A. Vedaldi. Fine-grained visual classification of
aircraft. Technical report, 2013.

- 648 Leland McInnes, John Healy, and James Melville. Umap: Uniform manifold approximation and
649 projection for dimension reduction. *arXiv preprint arXiv:1802.03426*, 2018.
650
- 651 John P Miller, Rohan Taori, Aditi Raghunathan, Shiori Sagawa, Pang Wei Koh, Vaishaal Shankar,
652 Percy Liang, Yair Carmon, and Ludwig Schmidt. Accuracy on the line: on the strong correlation
653 between out-of-distribution and in-distribution generalization. In *International conference on*
654 *machine learning*, pp. 7721–7735. PMLR, 2021.
- 655 Norman Mu, Alexander Kirillov, David Wagner, and Saining Xie. Slip: Self-supervision meets
656 language-image pre-training. In *European conference on computer vision*, pp. 529–544. Springer,
657 2022.
658
- 659 Yuval Netzer, Tao Wang, Adam Coates, Alessandro Bissacco, Baolin Wu, Andrew Y Ng, et al.
660 Reading digits in natural images with unsupervised feature learning. In *NIPS workshop on deep*
661 *learning and unsupervised feature learning*, volume 2011, pp. 7. Granada, Spain, 2011.
662
- 663 Changdae Oh, Junhyuk So, Hoyoon Byun, YongTaek Lim, Minchul Shin, Jong-June Jeon, and
664 Kyungwoo Song. Geodesic multi-modal mixup for robust fine-tuning. *Advances in Neural Infor-*
665 *mation Processing Systems*, 36, 2024.
- 666 Aaron van den Oord, Yazhe Li, and Oriol Vinyals. Representation learning with contrastive predic-
667 tive coding. *arXiv preprint arXiv:1807.03748*, 2018.
668
- 669 Omkar M Parkhi, Andrea Vedaldi, Andrew Zisserman, and CV Jawahar. Cats and dogs. In *2012*
670 *IEEE conference on computer vision and pattern recognition*, pp. 3498–3505. IEEE, 2012.
671
- 672 Robin L Plackett. The analysis of permutations. *Journal of the Royal Statistical Society Series C:*
673 *Applied Statistics*, 24(2):193–202, 1975.
- 674 Bryan A Plummer, Liwei Wang, Chris M Cervantes, Juan C Caicedo, Julia Hockenmaier, and Svet-
675 lana Lazebnik. Flickr30k entities: Collecting region-to-phrase correspondences for richer image-
676 to-sentence models. In *Proceedings of the IEEE international conference on computer vision*, pp.
677 2641–2649, 2015.
678
- 679 Farhad Pourpanah, Moloud Abdar, Yuxuan Luo, Xinlei Zhou, Ran Wang, Chee Peng Lim, Xi-
680 Zhao Wang, and QM Jonathan Wu. A review of generalized zero-shot learning methods. *IEEE*
681 *transactions on pattern analysis and machine intelligence*, 45(4):4051–4070, 2022.
682
- 683 Alec Radford, Jong Wook Kim, Chris Hallacy, Aditya Ramesh, Gabriel Goh, Sandhini Agarwal,
684 Girish Sastry, Amanda Askell, Pamela Mishkin, Jack Clark, et al. Learning transferable visual
685 models from natural language supervision. In *International conference on machine learning*, pp.
686 8748–8763. PMLR, 2021.
- 687 Aditya Ramesh, Mikhail Pavlov, Gabriel Goh, Scott Gray, Chelsea Voss, Alec Radford, Mark Chen,
688 and Ilya Sutskever. Zero-shot text-to-image generation. In *International conference on machine*
689 *learning*, pp. 8821–8831. Pmlr, 2021.
690
- 691 Benjamin Recht, Rebecca Roelofs, Ludwig Schmidt, and Vaishaal Shankar. Do imagenet classifiers
692 generalize to imagenet? In *International conference on machine learning*, pp. 5389–5400. PMLR,
693 2019.
- 694 Olga Russakovsky, Jia Deng, Hao Su, Jonathan Krause, Sanjeev Satheesh, Sean Ma, Zhiheng
695 Huang, Andrej Karpathy, Aditya Khosla, Michael Bernstein, Alexander C. Berg, and Li Fei-Fei.
696 ImageNet Large Scale Visual Recognition Challenge. *International Journal of Computer Vision*
697 (*IJCV*), 115(3):211–252, 2015. doi: 10.1007/s11263-015-0816-y.
698
- 699 Piyush Sharma, Nan Ding, Sebastian Goodman, and Radu Soricut. Conceptual captions: A cleaned,
700 hypernymed, image alt-text dataset for automatic image captioning. In *Proceedings of the 56th*
701 *Annual Meeting of the Association for Computational Linguistics (Volume 1: Long Papers)*, pp.
2556–2565, 2018.

- 702 Amanpreet Singh, Ronghang Hu, Vedanuj Goswami, Guillaume Couairon, Wojciech Galuba, Mar-
703 cus Rohrbach, and Douwe Kiela. Flava: A foundational language and vision alignment model.
704 In *Proceedings of the IEEE/CVF Conference on Computer Vision and Pattern Recognition*, pp.
705 15638–15650, 2022.
- 706 Richard Socher, Alex Perelygin, Jean Wu, Jason Chuang, Christopher D Manning, Andrew Y Ng,
707 and Christopher Potts. Recursive deep models for semantic compositionality over a sentiment
708 treebank. In *Proceedings of the 2013 conference on empirical methods in natural language pro-
709 cessing*, pp. 1631–1642, 2013.
- 710 Siddharth Srivastava and Gaurav Sharma. Omnivec: Learning robust representations with cross
711 modal sharing. In *Proceedings of the IEEE/CVF Winter Conference on Applications of Computer
712 Vision*, pp. 1236–1248, 2024.
- 713 J. Stallkamp, M. Schlipsing, J. Salmen, and C. Igel. Man vs. computer: Benchmarking machine
714 learning algorithms for traffic sign recognition. *Neural Networks*, (0):–, 2012. ISSN 0893-6080.
715 doi: 10.1016/j.neunet.2012.02.016. URL [http://www.sciencedirect.com/science/
716 article/pii/S0893608012000457](http://www.sciencedirect.com/science/article/pii/S0893608012000457).
- 717
718 Ajinkya Tejanekar, Maziar Sanjabi, Bichen Wu, Saining Xie, Madian Khabsa, Hamed Pirsiavash,
719 and Hamed Firooz. A fistful of words: Learning transferable visual models from bag-of-words
720 supervision. *arXiv preprint arXiv:2112.13884*, 2021.
- 721
722 Bart Thomee, David A. Shamma, Gerald Friedland, Benjamin Elizalde, Karl Ni, Douglas Poland,
723 Damian Borth, and Li-Jia Li. Yfcc100m: the new data in multimedia research. *Commun. ACM*,
724 59(2):64–73, January 2016. ISSN 0001-0782. doi: 10.1145/2812802. URL [https://doi.
725 org/10.1145/2812802](https://doi.org/10.1145/2812802).
- 726
727 Athanasios Voulodimos, Nikolaos Doulamis, Anastasios Doulamis, and Eftychios Protopapadakis.
728 Deep learning for computer vision: A brief review. *Computational intelligence and neuroscience*,
729 2018, 2018.
- 730 Haohan Wang, Songwei Ge, Zachary Lipton, and Eric P Xing. Learning robust global representa-
731 tions by penalizing local predictive power. *Advances in Neural Information Processing Systems*,
732 32, 2019.
- 733
734 Tan Wang, Kevin Lin, Linjie Li, Chung-Ching Lin, Zhengyuan Yang, Hanwang Zhang, Zicheng Liu,
735 and Lijuan Wang. Equivariant similarity for vision-language foundation models. In *Proceedings
736 of the IEEE/CVF International Conference on Computer Vision*, pp. 11998–12008, 2023.
- 737
738 Tongzhou Wang and Phillip Isola. Understanding contrastive representation learning through align-
739 ment and uniformity on the hypersphere. In *International conference on machine learning*, pp.
9929–9939. PMLR, 2020.
- 740
741 Kaicheng Yang, Jiankang Deng, Xiang An, Jiawei Li, Ziyong Feng, Jia Guo, Jing Yang, and
742 Tongliang Liu. Alip: Adaptive language-image pre-training with synthetic caption. In *Proceed-
743 ings of the IEEE/CVF International Conference on Computer Vision*, pp. 2922–2931, 2023.
- 744
745 Lewei Yao, Runhui Huang, Lu Hou, Guansong Lu, Minzhe Niu, Hang Xu, Xiaodan Liang, Zhenguo
746 Li, Xin Jiang, and Chunjing Xu. Filip: Fine-grained interactive language-image pre-training.
arXiv preprint arXiv:2111.07783, 2021.
- 747
748 Zhuokai Zhao, Harish Palani, Tianyi Liu, Lena Evans, and Ruth Toner. Multi-modality guidance
749 network for missing modality inference. *arXiv preprint arXiv:2309.03452*, 2023.
- 750
751
752
753
754
755

756 APPENDIX

757

758 A TRAINING PROCEDURES

759

760 A.1 IMPLEMENTATION DETAILS

761

762 For CLIP (Radford et al., 2021), we use the official implementation released by OpenAI¹. And for

763 ALIP (Yang et al., 2023), we also use the official implementation released by the paper authors². As

764 the proposed RANKCLIP essentially shares the same model architecture (separate vision, text en-

765 coders, projection layer, and a classification head) as CLIP, we build upon the CLIP code repository

766 for our model construction³. We set the scaling parameters for cross-modal (λ_c) and in-modal (λ_i)

767 ranking consistency to 1/16 and 1/16 respectively throughout all the experiments unless otherwise

768 noted. All CLIP, ALIP and RANKCLIP models are initialized from scratch without loading any

769 existing weights. And the embedding sizes for both modalities all project to 1024 across the three

770 models.

771 A.2 TRAINING PARAMETERS

772 Following CLIP (Radford et al., 2021), we adopt the ResNet-50 (He et al., 2016) and transformer

773 architectures (Devlin et al., 2018) for image and text encoding, respectively. Training is conducted

774 from scratch over 64 epochs using a single NVIDIA A100 GPU, with a batch size of 512, an initial

775 learning rate of 0.0005 employing cosine scheduling, and 10,000 warm-up steps.

776

777 A.3 TRAINING TIME CONSUMPTION

778 we conducted the experiments using the same hardware specifications. The table below shows the

779 time consumption for training our RankCLIP and CLIP models with 50K samples from CC3M using

780 a single NVIDIA A100 GPU.

781

782 Table 8: Training Details

783

	Time consumption	Dataset size	epochs	batch_size	model_name
CLIP	1d 2h 54m 48s	50K	64	512	RN50
RANKCLIP	1d 1h 4m 23s	50K	64	512	RN50

784

785

786

787

788 As shown in the table, the difference in time consumption is negligible. Interestingly, our method is

789 slightly faster than CLIP, but we think it may be attributed to hardware optimizations or variance.

790

791

792

793

794

795

796

797

798

799

800

801

802

803

804

805

806

807

808 ¹CLIP repository on GitHub: <https://github.com/openai/CLIP>.

809 ²ALIP repository on GitHub: <https://github.com/deepglint/ALIP>.

³RANKCLIP repository will be released upon acceptance.